Hollow Nanoparticles

DOI: 10.1002/anie.200700677

Synthesis and Characterization of Monodisperse Hollow Fe_3O_4 Nanoparticles**

*Sheng Peng and Shouheng Sun**

Hollow nanoparticles with controlled interior void and shell thickness are an important class of nanoporous materials. With large surface area and low material density, these nanoparticles could serve as ideal building blocks for fabrication of lightweight structural materials and for catalysis, nanoelectronics, and drug-delivery applications.[1] Recent progress has shown that hollow nanostructures can be readily synthesized by using the nanoscale Kirkendall effect.[2] This effect was initially proposed to describe the formation of voids at the interface of two bulk materials due to their different interdiffusion rates.[3] In a nanoparticle system, the Kirkendall effect refers to preferred outward elemental diffusion leading to a net material flux across the spherical interface and the consequent formation of a single void at the center.[4] Since the first report on the preparation of hollow CoS (CoO) nanoparticles by sulfidation (oxidation) of Co nanoparticles with exploitation of the Kirkendall effect,[5] several different kinds of hollow nanoparticles have been made by a similar approach. These include hollow CoSe nanoparticles from solution-phase selenization of Co nanoparticles[5,6] and hollow transition metal phosphide nanoparticles from reactions between metal nanoparticles and trioctylphosphane.[7] Hollow magnetic iron oxide nanoparticles have also been reported, but they were prepared by gas-phase oxidation[8] or electron-beam irradiation[9] of Fe nanoparticles, unsuitable for solution-phase self-assembly, surface functionalization, and encapsulation applications.

Here we report a facile solution-phase synthesis of monodisperse hollow Fe_3O_4 nanoparticles by controlled oxidation of Fe–Fe_3O_4 nanoparticles. We demonstrate that hollow nanoparticles with controllable size are formed due to the nanoscale Kirkendall effect, and the synthesis can be readily extended to produce various core–shell–void nanoparticles. We recently succeeded in synthesizing Fe nanoparticles by thermal decomposition of $[Fe(CO)_5]$ in the presence of oleylamine.[10] The Fe nanoparticles were not chemically stable, and oxidation when exposed to air gave core–shell Fe–Fe_3O_4 structures with both Fe and Fe_3O_4 in the amorphous state. Controlled oxidation of these core–shell nanoparticles in the presence of the oxygen-transfer reagent trimethylamine *N*-oxide (Me_3NO) led to the formation of intermediate core–shell–void Fe–Fe_3O_4, and further to hollow Fe_3O_4 nanoparticles (Scheme 1). The controlled oxidation

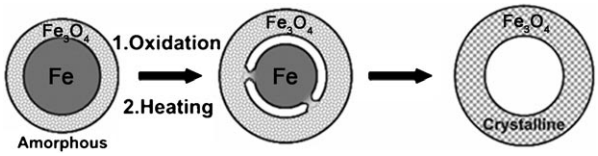

Scheme 1. Synthesis of core–shell–void Fe–Fe_3O_4 and hollow Fe_3O_4 nanoparticles from Fe–Fe_3O_4 nanoparticle seeds.

gave an Fe_3O_4 shell that contained polycrystalline Fe_3O_4 grains. The hollow nanoparticles prepared by the current synthesis are readily dispersed in various solvents, such as hexane, cyclohexane, toluene, and chloroform, and this facilitates their self-assembly into low-density porous nanostructures and surface functionalization.

The hollow Fe_3O_4 nanoparticles were prepared by controlled oxidation of amorphous core–shell Fe–Fe_3O_4 nanoparticles. The core–shell particles were obtained by high-temperature solution-phase decomposition of $[Fe(CO)_5]$ and air oxidation of the amorphous Fe nanoparticles at room temperature.[10] Figure 1a shows the transmission electron

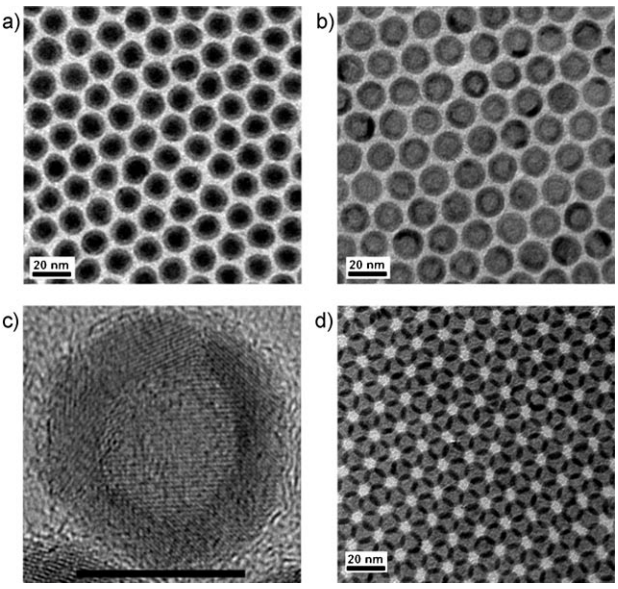

Figure 1. TEM images: a) 13-nm Fe–Fe_3O_4 nanoparticle seeds, b) 16-nm hollow Fe_3O_4 nanoparticles, c) a single hollow Fe_3O_4 nanoparticle (scale bar 10 nm), and d) a superlattice array of the hollow Fe_3O_4 nanoparticles.

[*] S. Peng, Prof. S. Sun
Department of Chemistry
Brown University
Providence, Rhode Island 02912 (USA)
Fax: (+1) 401-863-9046
E-mail: ssun@brown.edu

[**] The work was supported by NSF/DMR 0606264.

Supporting information for this article is available on the WWW under http://www.angewandte.org or from the author.

microscopy (TEM) image of the 8-nm/2.5-nm Fe–Fe_3O_4 nanoparticles. To make hollow Fe_3O_4 nanoparticles, a mixture of 20 mL of 1-octadecene and 30 mg of Me_3NO was stirred and heated to 130 °C under a constant Ar flow for 1 h. A dispersion of 80 mg of 8-nm/2.5-nm Fe–Fe_3O_4 nanoparticles in hexane was added to the mixture. The reactants were kept at 130 °C for 2 h to remove hexane and then heated at 210 °C for 2 h before cooling to room temperature. Hollow Fe_3O_4 nanoparticles (80 % yield) were precipitated by adding 2-propanol followed by centrifugation and washing with ethanol. The nanoparticles were dispersed in hexane for further use.

Figure 1 b shows a TEM image of hollow Fe_3O_4 nanoparticles with a standard deviation of less than 7 %. The overall diameter of the particles is around 16 nm. This represents a 3-nm increase compared to the 13-nm starting Fe–Fe_3O_4 nanoparticles. The oxide shell in the hollow structure is around 3.5 nm thick. The high-resolution TEM (HRTEM) image of a single hollow Fe_3O_4 nanoparticle shows that the shell contains multiple crystal domains (Figure 1 c). Slow evaporation of the dodecane dispersion of the hollow nanoparticles (with a concentration of ca. 0.2 mg mL^{-1}) on an amorphous-carbon-coated copper grid at 60 °C gave a large-area self-assembled superlattice with the particles in hexagonal close packing. Figure 1 d shows a TEM image of a small area of the superlattice array. Selected-area electron diffraction (SAED) of the superlattice showed a typical ring pattern (see the Supporting Information), indicative of no structural alignment in the array. This is consistent with the HTREM observation that the shell consists of polycrystalline Fe_3O_4 which may disrupt any alignment potential of the particles.

The powder X-ray diffraction (XRD) pattern of the 13-nm Fe–Fe_3O_4 nanoparticle seeds shows no diffraction peak (Figure 2 a), but the diffraction pattern of the hollow nanoparticles is consistent with that of the magnetite Fe_3O_4 phase (Figure 2 b). The Fe_3O_4 phase was further characterized by its thermal stability under high-temperature annealing condition (500 °C under Ar for 2 h), as shown in Figure 2 c.[11] Furthermore, the XRD peaks in Figure 2 c do not show obvious change in width compared to those in Figure 2 b, that is, the Fe_3O_4 shell is structurally stable during the annealing process. The polycrystalline nature of the Fe_3O_4 shell is revealed both in Figure 2 b and 2 c. The broad diffraction peaks originate from the small grain sizes of the Fe_3O_4 particles within the shell structure, which is in sharp contrast to the narrow diffraction peaks observed from the solid 16-nm Fe_3O_4 nanocrystals (Figure 2 d). This is consistent with the HRTEM analysis in Figure 1 c that the shell contains small polycrystalline Fe_3O_4 grains. By annealing the nanoparticles in air at 300 °C for 8 h, the as-synthesized 16-nm hollow Fe_3O_4 nanoparticles can be transformed into γ-Fe_2O_3 without significant morphological change. Hollow Fe_3O_4 nanoparticles with tunable sizes from 10 to 20 nm can be obtained by oxidizing smaller or bigger Fe–Fe_3O_4 nanoparticle seeds (see Supporting Information).

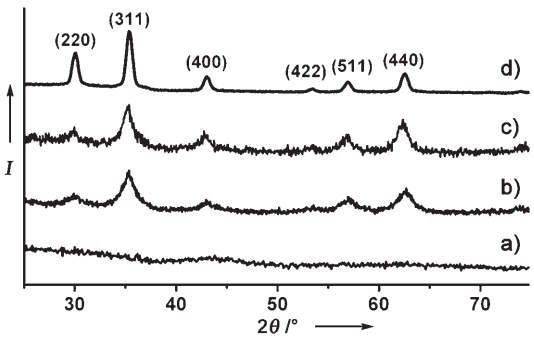

Figure 2. XRD patterns of a) 13-nm Fe–Fe_3O_4 nanoparticle seeds, b) 16-nm hollow Fe_3O_4 nanoparticles, c) the particles in (b) after annealing at 500 °C under Ar for 2 h, and d) 16-nm solid Fe_3O_4 nanoparticles.

To study void evolution in the amorphous Fe–Fe_3O_4 nanoparticles during the controlled oxidation process, we took aliquots of reaction mixtures at different time during the reaction, quickly precipitated the nanoparticles, and redispersed them into hexane for preparation of TEM samples. Figure 3 shows a series of TEM images of the nanoparticles

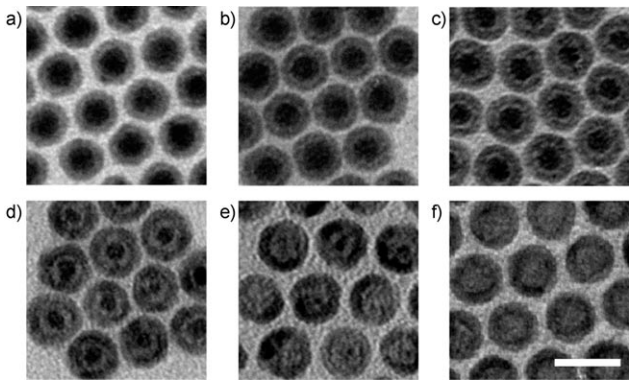

Figure 3. TEM images of various Fe–Fe_3O_4 and hollow Fe_3O_4 nanoparticles: a) Fe–Fe_3O_4 nanoparticle seeds; b)–e) core–shell–void Fe–Fe_3O_4 nanoparticles obtained from the reaction at b) 130 °C for 1 h, c) 130 °C for 2 h, d) 210 °C for 40 min, e) 210 °C for 80 min, f) 210 °C for 120 min; scale bar 20 nm.

from different reaction conditions. As synthesized, the core–shell Fe–Fe_3O_4 nanoparticles showed no visible gap between Fe and Fe_3O_4 (Figure 3 a). A gap between core and shell of less than 1 nm developed after heating the seed nanoparticles at 130 °C for 1 h (Figure 3 b). The gap broadened to about 1.5 nm after 2 h of heating (Figure 3 c). The rate of core consumption and gap broadening is greatly enhanced at higher reaction temperature. After heating at 210 °C for 40 min, the core size shrunk to about 5 nm and the gap grew to 2.5 nm (Figure 3 d). The cores were almost depleted after heating at 210 °C for 80 min (Figure 3 e). Finally, all of the cores disappeared after heating for 2 h at 210 °C, leaving nearly spherical voids in the center of the nanoparticles (Figure 3 f). The final void diameter of about 9 nm was slightly larger than that of the original 8-nm Fe cores. The Fe_3O_4 layer thickness was increased from 2.5 nm in the amorphous seeds to 3.5 nm in the final hollow nanoparticles.

The observations made in the process of forming hollow Fe_3O_4 nanoparticles reveal that the Kirkendall effect directs

the controlled oxidation of Fe–Fe_3O_4, in which Fe metal diffuses faster outward than oxygen does inward, and Fe_3O_4 collects at the metal–oxide interface rather than in the interior of the core. This is consistent with the observation that the metal is the faster diffusing component in a diffusion couple of metal and oxygen.[12] The TEM images in Figure 3c and d also show an Fe bridge (or several Fe bridges) between core and shell, which is similar to what has been observed in the synthesis of hollow CoS nanoparticles.[5] The bridge seems to provide a fast transport path for outward diffusion of Fe atoms and it stays connected to the shell until the core is completely consumed. This Kirkendall effect was not observed in the previous oxidation of Fe nanoparticles by Me_3NO, in which, without exposure to air, the Fe nanoparticles were directly mixed with Me_3NO to give solid iron oxide nanoparticles.[13] We consider the initial air oxidation of the Fe nanoparticles to form amorphous Fe–Fe_3O_4 the key to the unbalanced interfacial diffusion of oxygen and Fe atoms during the oxidation process.

The time needed for complete consumption of the Fe core in the Fe–Fe_3O_4 structure and the morphology of the shell are dependent on the reaction temperature. When 13-nm Fe–Fe_3O_4 nanoparticles were incubated with Me_3NO at 130 °C, complete oxidation was not achieved until 8 h later. The resultant nanoparticles were uniform hollow spheres (Figure 4a). Studies by HRTEM (Figure 4b) and XRD (see the Supporting Information) revealed that the hollow nanoparticles are amorphous, that is, Fe_3O_4 in the shell structure does not crystallize at 130 °C. When the mixture of 13-nm Fe–Fe_3O_4 and Me_3NO was heated at 250 °C, hollow nanoparticles were obtained after only 10 min of heating. The hollow nanoparticles synthesized at this temperature have similar polycrystalline structure to those produced at 210 °C, but show more faceted morphology within the shell structure (Figure 4c and 4d). It seems that, at high reaction temperature, Fe_3O_4 tends to crystallize in bigger grains.

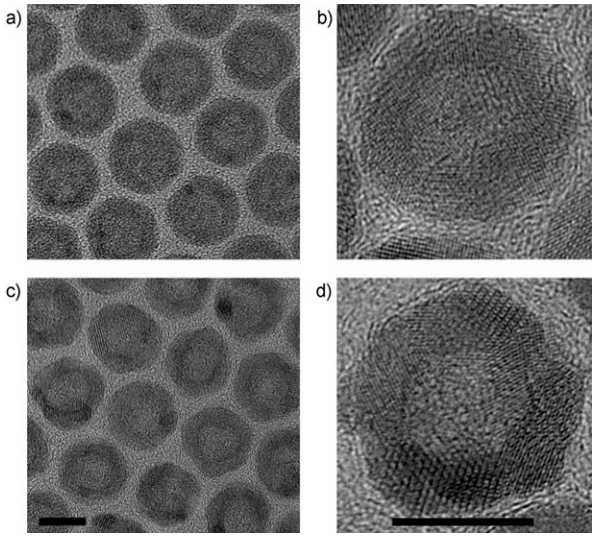

Figure 4. TEM images of the hollow Fe_3O_4 nanoparticles synthesized at a, b) 130 °C for 8 h and c, d) 250 °C for 10 min; scale bars 10 nm.

The hollow Fe_3O_4 nanoparticles are superparamagnetic at room temperature. The particles obtained at 210 °C have a saturation moment M of 47.9 emu g^{-1} (Figure 5a), which is about 60% of that of 16-nm solid Fe_3O_4 nanoparticles (83 emu g^{-1}) (Figure 5b).[11] Unlike solid nanoparticles, the hollow particles can not be saturated magnetically in fields as high as 1 T. This reflects the fact that the hollow nanoparticles, like small magnetic nanoparticles, are subject to thermal agitation and surface spin-canting effects.[14] This further proves that the shell contains small Fe_3O_4 magnetic grains, as concluded from both HRTEM and XRD studies.

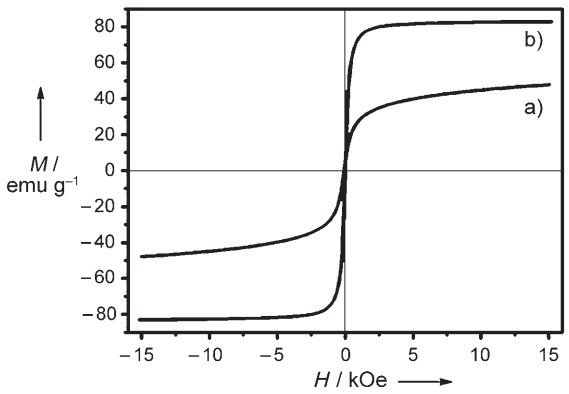

Figure 5. Room-temperature hysteresis loops of a) 16-nm hollow Fe_3O_4 nanoparticles shown in Figure 1b and b) 16-nm solid Fe_3O_4 nanoparticles.

In conclusion, we have succeeded in preparing monodisperse hollow Fe_3O_4 nanoparticles by controlled oxidation of amorphous core–shell Fe–Fe_3O_4 nanoparticles. The Fe_3O_4 shell can be controlled to be amorphous or polycrystalline by means of the heating conditions. Self-assembly of the monodisperse hollow Fe_3O_4 nanoparticles leads to superlattice arrays. Using similar reaction conditions, we have also isolated core–shell–void Fe–Fe_3O_4 nanoparticles. The synthesis offers a general approach to hollow iron oxide and core–shell–void Fe–Fe_3O_4 nanoparticles by exploiting the nanoscale Kirkendall effect. This methodology is also extendable to produce other types of hollow or core–shell–void transition-metal oxide nanoparticles. We are currently exploring the syntheses of magnetic hollow and core–shell–void nanoparticles with controlled porosity and conductivity in shell and magnetic moment density in core for catalysis and high-frequency electromagnetic device applications.

Received: February 13, 2007
Published online: April 27, 2007

Keywords: iron · magnetic properties · nanostructures · oxidation · oxides

[1] a) P. T. Tanev, M. Chibwe, T. J. Pinnavaia, *Nature* **1994**, *368*, 321–323; b) F. Schüth, *Annu. Rev. Mater. Res.* **2005**, *35*, 209–238; c) J. Erlebacher, M. J. Aziz, A. Karma, N. Dimitrov, K. Sieradzki, *Nature* **2001**, *410*, 450–453; d) O. D. Velev, E. W. Kaler, *Adv. Mater.* **2000**, *12*, 531–534; e) F. Caruso, R. A. Caruso, H.

Möhwald, *Science* **1998**, *282*, 1111 – 1114; f) S. H. Im, U. Jeong, Y. Xia, *Nat. Mater.* **2005**, *4*, 671 – 675.
[2] a) H. C. Zeng, *J. Mater. Chem.* **2006**, *16*, 649 – 662; b) Y. Wang, L. Cai, Y. Xia, *Adv. Mater.* **2005**, *17*, 473 – 477; c) Y. Yin, C. Erdonmez, S. Aloni, A. P. Alivisatos, *J. Am. Chem. Soc.* **2006**, *128*, 12671 – 12673; d) Y. Chang, M. L. Lye, H. C. Zeng, *Langmuir* **2005**, *21*, 3746 – 3748; e) L. Zhang, J. C. Yu, Z. Zheng, C. W. Leung, *Chem. Commun.* **2005**, 2683 – 2685; f) H. Jin fan, M. Knez, R. Scholz, K. Nielsch, E. Pippel, D. Hesse, M. Zacharias, U. Gösele, *Nat. Mater.* **2006**, *5*, 627 – 631; g) Q. Li, R. M. Penner, *Nano Lett.* **2005**, *5*, 1720 – 1725; h) H. Cao, X. Qian, J. Zai, J. Yin, Z. Zhu, *Chem. Commun.* **2006**, 4548 – 4550.
[3] A. D. Smigelskas, E. O. Kirkendall, *Trans. Am. Inst. Min. Metall. Pet. Eng.* **1947**, *171*, 130 – 142.
[4] a) K. N. Tu, U. Gösele, *Appl. Phys. Lett.* **2005**, *86*, 093111; b) A. M. Gusak, T. V. Zaporozhets, K. N. Tu, U. Gösele, *Philos. Mag.* **2005**, *85*, 4445 – 4464.
[5] a) Y. Yin, R. M. Rioux, C. K. Erdonmez, S. Hughes, G. A. Somorjai, A. P. Alivisatos, *Science* **2004**, *304*, 711 – 714; b) Y. Yin, C. K. Erdonmez, A. Cabot, S. Hughes, A. P. Alivisatos, *Adv. Funct. Mater.* **2006**, *16*, 1389 – 1399.
[6] a) J. Gao, B. Zhang, X. Zhang, B. Xu, *Angew. Chem.* **2006**, *118*, 1242 – 1245; *Angew. Chem. Int. Ed.* **2006**, *45*, 1220 – 1223; b) J. Gao, G. Liang, B. Zhang, Y. Kuang, X. Zhang, B. Xu, *J. Am. Chem. Soc.* **2007**, *129*, 1428 – 1433.
[7] a) R.-K. Chiang, R.-T. Chiang, *Inorg. Chem.* **2007**, *46*, 369 – 371; b) A. E. Henkes, Y. Vasquez, R. E. Schaak, *J. Am. Chem. Soc.* **2007**, *129*, 1896 – 1897.
[8] C. M. Wang, D. R. Baer, L. E. Thomas, J. E. Amonette, J. Antony, Y. Qiang, G. Duscher, *J. Appl. Phys.* **2005**, *98*, 094308.
[9] a) A. H. Latham, M. J. Wilson, P. Schiffer, M. E. Williams, *J. Am. Chem. Soc.* **2006**, *128*, 12632 – 12633; b) D. Farrell, S. A. Majetich, J. P. Wilcoxon, *J. Phys. Chem. B* **2003**, *107*, 11022 – 11030.
[10] S. Peng, C. Wang, J. Xie, S. Sun, *J. Am. Chem. Soc.* **2006**, *128*, 10676 – 10677.
[11] S. Sun, H. Zen, D. B. Robinson, S. Raoux, P. M. Rice, S. X. Wang, G. Li, *J. Am. Chem. Soc.* **2004**, *126*, 273 – 279.
[12] G. W. Leibbrandt, G. Hoogers, F. H. P. M. Habraken, *Phys. Rev. Lett.* **1992**, *68*, 1947 – 1950.
[13] T. Hyeon, S. S. Lee, J. Park, Y. Chung, H. B. Na, *J. Am. Chem. Soc.* **2001**, *123*, 12798 – 12801.
[14] B. Martínez, X. Obradors, L. Balcells, A. Rouanet, C. Monty, *Phys. Rev. Lett.* **1998**, *80*, 181 – 184.

